

Inside LaTeX2e kernel

Sigitas Tolušis*

VTEX Ltd., Akademijos 4, 2600 Vilnius, Lithuania

E-mail: vtex@post.omnitel.net

Abstract

The standard LaTeX2e typesetting system is quite flexible and allows covering most of customer needs but on other hand it still has some restrictions on formatting the page layout, especially in twocolumn mode. I would like to present some packages based on modified low level LaTeX2e kernel macros. Using these packages is possible: to balance columns on the last page in twocolumn mode; to place double-column float at bottom of page; to place footnotes below the bottom floats; to insert some wide onecolumn material in any place of twocolumn page and to do some other things.

Contents

1	Introduction	2
2	Typesetting in onecolumn	2
2.1	Floating baselineskip	2
2.2	Footnotes below the floats	3
2.3	Different pagestyles for text and float pages	3
2.4	Multipage tabular	3
3	Typesetting in twocolumn	4
3.1	Column balancing at last page	4
3.2	Dblfloats at bottom	5
3.3	Mixing onecolumn and twocolumn modes at any place of page	5

*E-mail: sigitas@vtx.lt

4 Conclusions

1 Introduction

Typesetting a lot of papers in the typesetting company is quite different from personal typesetting of a few articles by one person. Author formatting his own article takes into account the L^AT_EX capabilities. If he do not like appearance of the footnote below the bottom float, he could change the text to avoid it.

Contrary, the typesetting company must implement publisher's requirements. At VTeX typesetting company we designed some packages to get around some L^AT_EX limitations.

2 Typesetting in onecolumn

Typesetting in one column is very well supported by standard L^AT_EX but we still find some situations for extending its output. I will shortly introduce to some of them.

2.1 Floating baselineskip

Using a baselineskip with stretch and shrink component's is not recommended by Grand Wizard. However, to avoid bad page breaks usually it's necessary.

Try to use `\fontsize{10pt}{12pt plus .1pt minus .1pt} \selectfont`. To your surprise `\baselinestretch` still remains fixed (in our case 12pt). Any stretch or shrink is removed. It is effect of the fact that any glue with prefixing number (in this case `\baselinestretch`) is converted to dimension. The L^AT_EX defines `\baselinestretch` equal to 1. You can simply `\renewcommand{\baselinestretch}{}` or could use `stkernel` package.

The package `stkernel` provides possibility to save the baselineskip stretch and shrink. It is controlled by commands:

- `\setbaselinefloat` - enables baselineskip floating
- `\setbaselinefixed` - standard behaviour

The changes are made in L^AT_EX kernel macro `\set@fontsize`.

2.2 Footnotes below the floats

Footnotes in a page with bottom floats in any case looks ugly. The standard behaviour of L^AT_EX is to put footnotes above the bottom float. The same package *stkernel* provides two new commands:

- \fnbelowfloat - to put footnotes below the bottom floats
- \fnunderfloat - standard behaviour

It is based on changing the L^AT_EX kernel macro \@makecol.

2.3 Different pagestyles for text and float pages

It is common in publishing to use a different page style (running head and foot lines) to pages, occupied by landscape tables and figures. The fact that every float in standard L^AT_EX kernel is managed as element of separate insertion class allow us to identify each float and to specify any hook to each float on the document. This idea is used in the package *floatpag*¹ which is used to specify different pagestyles for ordinary text pages, float pages and even rotated floats pages. In the modified commands \@xfloat and \@xrotfloat the identification of the float takes place and modified command \@vtryfc executes the specific command for outputted floats.

For the end user these commands are provided:

- \floatpagestyle{...}
- \rotfloatpagestyle{...}
- \thisfloatpagestyle{...}

Extensions Using the same idea it is possible to write other extensions to float output, based on possibility to execute some commands for any specific or common float (or float type) in the document.

2.4 Multipage tabular

We have defined one more of existing multipage tabular environments *stabular*. The idea is quite different from existing solutions (as packages *supertab* and *longtable*), but quite simple. The modifications are based on the same tabular environment and internal macros except that tabular material is not put inside the box. In that case we have the same (or very similar) behaviour as standard tabular environment, but it is not restricted to one page. It is based on changed L^AT_EX kernel macros \@tabular and \@array. The solution is provided by package *stabular*. It also has some other modifications to tabular (just experimental).

¹Developed together with V. Statulevičius

3 Typesetting in twocolumn

With standard L^AT_EX we have possibility to typeset text in onecolumn or twocolumn mode, but the twocolumn mode has some restrictions to compare with onecolumn. Even more restrictions appear on mixing both modes together on the same page. What are the possibilities to typeset text in twocolumn mode? Actually, there are two of them (at least well known):

- twocolumn mode of standard L^AT_EX
- package *multicol* written by Frank Mittelbach

In any case the both solutions is not adapted in full range for typesetting text in twocolumn mode.

The main restrictions of standard twocolumn mode are:

- the columns are never balanced
- the mixing of onecolumn and twocolumn formatting on the same page is impossible

The main restrictions of *multicol* package are:

- missing support of floats (except dblfloats)
- partial support of standard footnotes output

So, the *multicol* is excellent tool for producing some twocolumn (three, four, etc.) formatting in standard onecolumn mode, but for typesetting full articles with a lot of floats and editing it cannot be used. It requires too much of handiwork.

We decided to use standard twocolumn mode with changed standard L^AT_EX output routines. I will briefly introduce to our experience in finding possible ways to some solutions.

3.1 Column balancing at last page

Standard L^AT_EX twocolumn mode output routine formats columns independently, putting the material in separate boxes. The idea for balancing columns is to split the lefcolumn box and add the split part of box to the top of rightcolumn box. For this purpose we use *flushend* package.

It redefines the L^AT_EX kernel macro `\@outputdblcol` for the last page and provides a few additional commands. After loading the package with the command `\usepackage{flushend}` the following commands can be used:

- `\flushend` (loaded by default) - enables balancing columns on last page
- `\raggedend` - disables balancing

- `\atColsBreak{...}` - inserts ... between the split part of the leftcolumn box and the top of rightcolumn box.
It helps to add some vertical adjustment.
- `\showcolsendlrule` - can be used for debugging

It is possible to influence the balancing of columns by adding positive or negative vertical skips just before the end of document.

Extensions Using the same idea and managing the contents of L^AT_EX kernel macro `\@outputdblcol` it can be extended for the balancing columns on any page of the document, not the last only.

3.2 Dblfloats at bottom

In standard L^AT_EX twocolumn mode it is possible to place star forms of floats (in other words dblfloats) only at the top of page, but sometimes customers have requirements to put such floats at the bottom of the page. The idea is to put the dblfloat material not on the top of the output box but on the bottom when standard L^AT_EX output routine is combining the dblfloat with the rest formatted text on the current page. For this purpose we use package *stkernel* (it contains also some other tools).

We can get such behaviour with redefining of the L^AT_EX kernel macro `\@combinedblfloats`.

The new command `\dblfloatsatbottom` switches the output mode for dblfloats from top placement to bottom. The side influence is that produced page will be longer by `\topskip`. To correct the situation it is necessary just to add `\vskip\topskip` at the end of dblfloat environment. Another inconvenience is that `\dblfloatsatbottom` command should be used at the page where actual float appears. Some problems can appear when on the same page other floats are placed also (the numbering problems).

Extensions It is not really user friendly solution. So it can be changed a bit by adding support for optional parameters [t] or [b] to dblfloat environment to manage the behaviour of dblfloat output place. In that case command `\dblfloatsatbottom` will disappear.

3.3 Mixing onecolumn and twocolumn modes at any place of page

There is no possibility to mix typesetting text in onecolumn and twocolumn modes on the same page using standard L^AT_EX . We use two different packages for managing proper typesetting in such cases:

- *cuted* - the provided environment `strip` balances previous text columns and starts one column mode. One column mode are not restricted to one page (text flow: 1,2,3,4,5)
- *midfloat* - the columns are cut at that place, no reformatting (text flow: 1,3,4,2,5)

1	2
3	
4	5

It is the most complicated packages in provided set and needs some extra investigation. We have used package *cuted* in "real life" and package *midfloat* still remains in our testing area of L^AT_EX extension possibilities. By using *cuted* package it is possible to place onecolumn material from any column, left or right, *midfloat* restricts it to left column only. So I will stay on explanation of the first one.

The package *cuted* is based on L^AT_EX "interrupt" mechanism using negative penalty value -100005. So the new environment is managed in the same way as other floats. Package redefines standard L^AT_EX macros `\@outputdblcol`, `\@specialoutput` and `\output`. It provides new environment:

- `strip` - for placing onecolumn text material in twocolumn page(s) (it is not restricted to one page).

and command:

- `\oldcolsbreak{...}` - for inserting ... in the merge place on the right column of reformatted text.

4 Conclusions

If you find these ideas and packages useful you can find these packages at:

<http://www.vtex.lt/tex/download/macros>

So, take it and enjoy in using them. We welcome any comments and remarks.

ing modified Boyden chambers (Elgebaly, Herbert, et al., 1987). Cell migration in response to the putative chemoattractants was expressed as

$$\text{maximum chemotactic response} = \left(\frac{\text{CI}_{\text{experimental}} - \text{CI}_{\text{HBSS}}}{\text{CI}_{\text{C5 fragment}} - \text{CI}_{\text{HBSS}}} \right) \times 100\%$$

where CI is the chemotactic index (distance traveled on the filter \times cell number), C5 fragment is the positive control for 100% chemotactic response, and HBSS is Hank's balanced salt solution (a blank with no attractant property).¹

[s3] Example

The effects of supernatants obtained from NaOH-treated bovine corneas on the migration of neutrophils or mononuclear cells in vitro are shown in Fig. 2. After 2 hr of incubation, significant levels of chemotactic activity for both cell types were detected. Less activity, however, was found in

¹Example of footnote output above the float

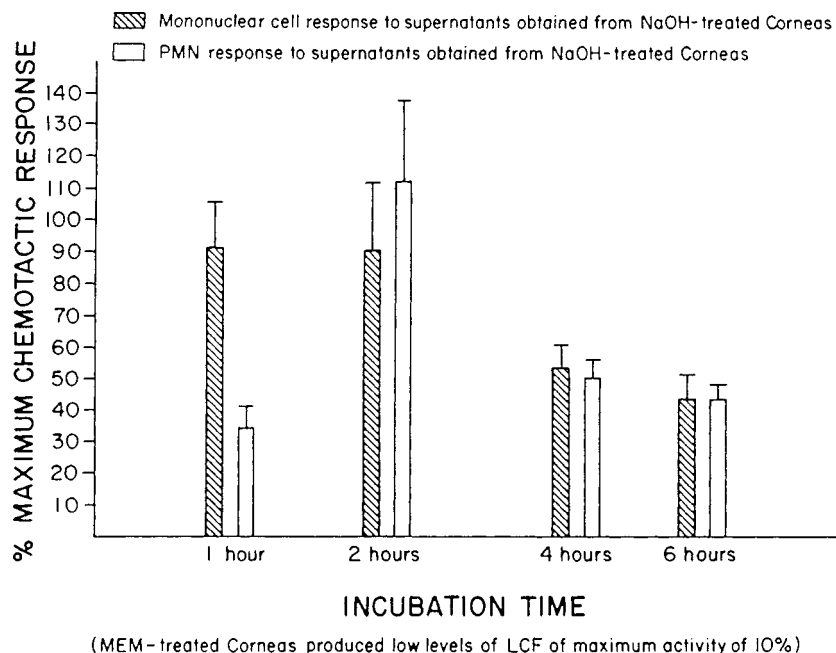


Figure 6.2. Mononuclear cell and neutrophil chemotactic activity present in supernatants of bovine corneas exposed to 1 N NaOH for 35 sec, washed once with MEM, and then incubated with MEM for 1, 2, 4, and 6 hr. The figure represents the mean of four experiments \pm standard deviation: \blacksquare mononuclear cell response to supernatants obtained from NaOH-treated corneas; \square PMN response to supernatants obtained from NaOH-treated corneas. (MEM-treated corneas produced low levels of LCF of maximum activity of 10%). (Reproduced with permission from Elgebaly, Downes, et al., 1987 and Oxford University Press.)

ing modified Boyden chambers (Elgebaly, Herbert, et al., 1987). Cell migration in response to the putative chemoattractants was expressed as

$$\text{maximum chemotactic response} = \left(\frac{\text{CI}_{\text{experimental}} - \text{CI}_{\text{HBSS}}}{\text{CI}_{\text{C5fragment}} - \text{CI}_{\text{HBSS}}} \right) \times 100\%$$

where CI is the chemotactic index (distance traveled on the filter \times cell number), C5 fragment is the positive control for 100% chemotactic response, and HBSS is Hank's balanced salt solution (a blank with no attractant property).¹

[s3] Example

The effects of supernatants obtained from NaOH-treated bovine corneas on the migration of neutrophils or mononuclear cells in vitro are shown in Fig. 2. After 2 hr of incubation, significant levels of chemotactic activity for both cell types were detected. Less activity, however, was found in

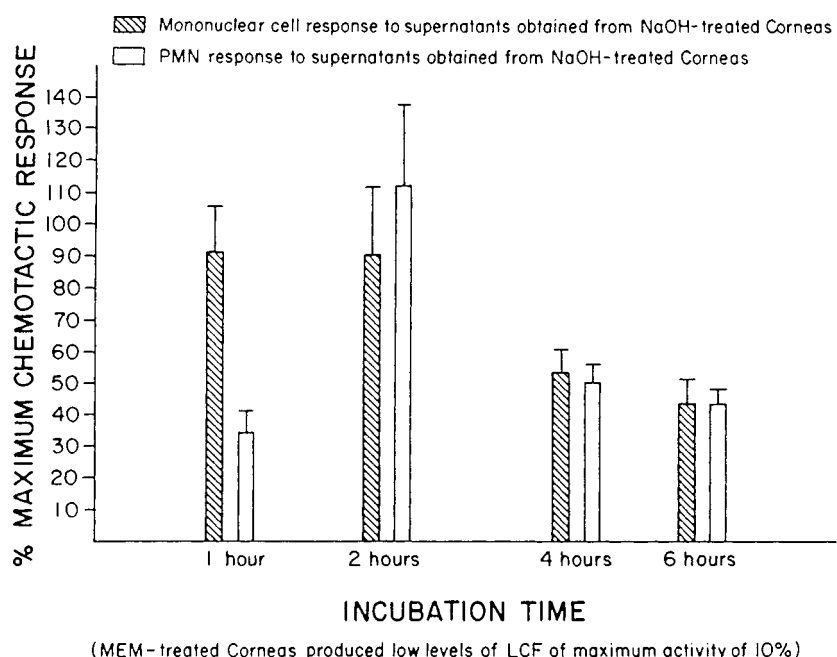


Figure 6.2. Mononuclear cell and neutrophil chemotactic activity present in supernatants of bovine corneas exposed to 1 N NaOH for 35 sec, washed once with MEM, and then incubated with MEM for 1, 2, 4, and 6 hr. The figure represents the mean of four experiments \pm standard deviation: \blacksquare mononuclear cell response to supernatants obtained from NaOH-treated corneas; \square PMN response to supernatants obtained from NaOH-treated corneas. (MEM-treated corneas produced low levels of LCF of maximum activity of 10%). (Reproduced with permission from Elgebaly, Downes, et al., 1987 and Oxford University Press.)

¹Example of footnote output below the float

ball; in other preparations, the endothelium and Descemet's membrane were scraped off after first removing the rear of the eyeball, removing the lens, and evertting the cornea over a second eyeball. Some corneas were used with both epithelium and Descemet's membrane removed. Holders, designed to allow contact of either or both surfaces with Tyrode solution or sodium lauryl sulfate (NaLS) solutions of various concentrations, were filled with Tyrode solution and placed in a Muir opacitometer. The voltage was adjusted to 2.5 V. The Tyrode solution was discarded and a cornea fixed in the chamber. Tyrode solution or NaLS solution was then placed on one or both sides of the cornea. The holder, with cornea and solutions, was placed again in the opacitometer and the voltage recorded (V1). Corneas were then incubated for 4.5 hr. The solutions on both sides of the cornea were then replaced with fresh Tyrode's solution and the voltage recorded again (V2). Since a drop in voltage indicates the development of opacity in the cornea, the results were expressed as percent opacity:

$$\left(\frac{V_1 - V_2}{V_1} \right) \times 100\%$$

where $V_1 - V_2 = 0$ represents zero opacity and $V_1 - V_2 = 2.5$ represents 100% opacity.

[s3] Examples

In one study (Muir, 1984), control corneas showed no opacity for 8 hr and then became more opaque over 24 hr. Care had to be taken to use fresh Tyrode solution as solutions became turbid with time. Sodium dodecyl sulfate (NaDS) at 1 mM caused almost complete opacity by 8 to 12 hr, whereas sodium lauryl sulfate (NaLS) at 1 mM caused opacity to fall more slowly, leveling off at 0.5 at 20 hr. Opacity with both surfactants was concentration-dependent, with NaDS much more potent as an irritant; this contrasts to its lower toxicity to cultured cells (Scaife, 1982).

Another study of isolated corneas exposed to NaLS (Igarashi, 1986) showed that opacity developed primarily in the stroma, in a concentration-dependent manner, and was greatest when epithelium and endothelium were removed. Igarashi (1986) thought that opacity was due to a reaction of NaLS with stromal proteins.

[s2] Corneal Cup Method

[s3] Leukocyte Chemotactic Factor Production

Corneas are prepared from fresh bovine eyes as illustrated in Fig. 1 (Elgebaly, Gillies, et al., 1985; Elgebaly, Downes, et al., 1987). The attached lens and most of the iris are removed and the resulting "corneal cup" is then washed twice in saline and maintained in cold minimal essential medium (MEM) until used. The cup is mounted in a paraffin well

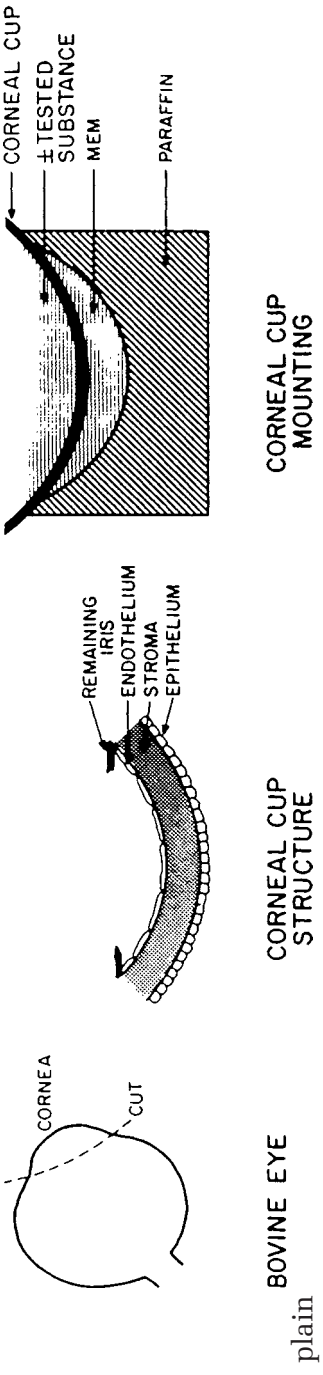


Figure 6.1.

Diagrammatic representation of the isolation and preparation of the cornea and the corneal cup model. (Reproduced with permission from Elgebaly, Downes, et al., 1987 and Oxford University Press.)

pression of acetylcholine receptor genes results, in part, from the regulation of transcription, which, in developing myotubes, is active in most sarcoplasmic nuclei but, in the adult, becomes restricted to the subjunctional “fundamental” nuclei. In the promoter of the receptor genes, distinct elements (NBox vs. EBox) control subjunctional transcription vs. activity-dependant extra-junctional repression. Posttranscriptional mechanisms include the conformational maturation of the receptor protein, its transit via a specialized *Golgi apparatus* (in the mature endplate), as its targeting, aggregation, metabolic stabilisation and immobilisation in the postsynaptic membrane.

Factors of neural origin involved in compartmentalized gene expression include calcitonin gene-related peptide, and “Acetylcholine Receptor Inducing Activity” (ARIA), a factor homologous to human heregulin and glial growth factor, which binds to tyrosine kinase receptors of the erb B_{2/3} family. A basal lamina component, the acetylcholine receptor aggregating factor, referred to as AGRIN, elicits acetylcholine receptor clusters formation and a cytoskeletal protein 43 K-Rapsyn contributes to its immobilisation and stabilisation in the postsynaptic membrane.

In the brain, nicotinic receptor genes are expressed exclusively in neurons and display different patterns of expression from highly restricted to a few nerve cells (α_2 -subunit) to wide spread ones (β_2 -subunit). Inactivation of β_2 -subunit gene by homologous recombination interferes with passive avoidance learning in the mouse. Nicotinic receptor binding drugs are considered as potential therapeutic agents in Alzheimer disease, Tourette’s syndrome and anxiety disorders. Correlations have been reported between cigarette smoking and protection against

ulcerative colitis and Parkinson’s disease. Nicotinic addiction plausibly involves high affinity nicotinic receptors associated with mid-brain dopaminergic neurons.

Further reading

- Changeux JP (1981): The acetylcholine receptor: An “allosteric” membrane protein. *Harv Lect* 75:85–254
 Changeux JP (1990): Functional architecture and dynamics of the nicotinic acetylcholine receptor: An allosteric ligand-gated ion channel. In: *Fidia Research Foundation Neuroscience Award Lectures, vol. 4*. Changeux JP, Llinas RR, Purves D, Bloom FE, eds. New York: Raven Press, pp. 21–168
 Changeux JP, Devillers-Thiéry A, Chemouilli P (1984): The acetylcholine receptor: An “allosteric” protein engaged in intracellular communication. *Science* 225:1335–1345
 Duclert A, Changeux JP (1995): Acetylcholine receptor gene expression at the developing neuromuscular junction. *Physiol Rev* 75:339–368
 Galzi JL, Changeux JP (1994): Neurotransmitter-gated ion channels as unconventional allosteric proteins. *Curr Opin Struct Biol* 4:554–565
 Hall ZW, Sanes JR (1993): Synaptic structure and development: The neuromuscular junction. *Cell/Neuron* 72:99–121
 Karlin A, Akabas MH (1995): Toward a structural basis for the function of nicotinic acetylcholine receptors and their cousins. *Neuron* 15:1231–1244
 Unwin N (1995): Acetylcholine receptor channel imaged in the open state. *Nature* 373:37–43

See also Acetylcholine; Neuromuscular junction; Neuronal receptors; Acetylcholine receptors, muscarinic; Acetylcholine receptors, nicotinic

Acetylcholine receptors, muscarinic

Robert S. Aronstam and Henry L. Puhl

Muscarinic receptors comprise one of the two classes of receptors for the neurotransmitter acetylcholine, nicotinic receptors comprising the other class. Muscarinic receptors are selectively activated by the alkaloid muscarine from the mushroom *Amanita muscaria*, and are blocked by *Belladonna* alkaloids, such as atropine and scopolamine (Figure 1). Muscarinic receptors are widely involved in the transduction of cholinergic signals in the central nervous system, autonomic ganglia, smooth muscles, and other parasympathetic end organs.

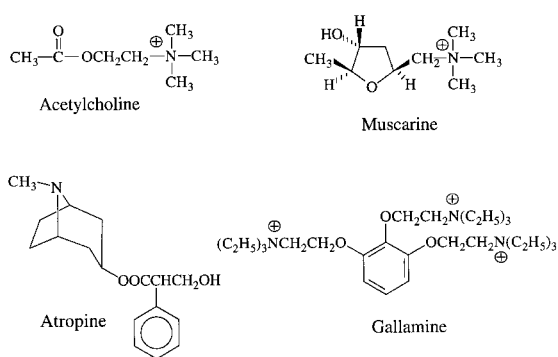


Figure 1. Structures of muscarinic ligands. Acetylcholine is the physiological agonist; muscarine and atropine are the prototypical agonist and antagonist which define the receptor class; gallamine is an allosteric receptor antagonist.

The history of muscarinic systems is intimately associated with the development of receptor theory and the discovery of neurotransmitter transmission. Muscarinic receptors are members of the superfamily of G protein-coupled receptors. Muscarinic receptors are related to the ion channel-containing nicotinic acetylcholine receptors only insofar as their physiological agonist is acetylcholine; muscarinic and nicotinic receptors share little similarity in their structure, physiological functions and pharmacology (except for a few close analogues of acetylcholine itself).

The genes for 5 subtypes of muscarinic receptors, m1–m5, were identified, cloned and sequenced between 1986 and 1990. These receptor subtypes differ in their distribution, pharmacology and signal transduction pathways (Table 1). This heterogeneity raises the possibility of selectively affecting specific muscarinic functions in the brain and other organs; accordingly, the pharmacology of muscarinic receptor subtypes has been the subject of intensive investigation. Unfortunately, the selectivity of antagonists for receptor subtypes rarely exceeds 10 fold. Properties of the different subtypes are summarized in Table 1. A schematic diagram of the human m2 receptor is presented as Figure 2.

1. Receptor structure

Muscarinic receptors are comprised of single polypeptides of 440–540 amino acids with an extracellular N-terminus and an intracellular C-terminus. Receptor genes contain a single exon.

Acetylcholine receptors, nicotinic

Edson X. Albuquerque

1. Introduction

The nicotinic acetylcholine receptor in vertebrate muscle was recognized nearly a century ago by Langley as a “receptive substance” for nicotine, long before the important role of this receptor in cholinergic neurotransmission was demonstrated. Similar receptors have been found on neurons of the central and peripheral nervous systems and in epithelial cells from a variety of species. Even though the nicotinic receptors exhibit diverse sensitivity to various pharmacological agents, they apparently are all physiologically stimulated by the neurotransmitter acetylcholine (ACh) and another endogenous substance, which exerts a positive allosteric effect on nicotinic receptors. After ACh and the putative transmitter are released from nerve terminals, these molecules diffuse across the synaptic cleft to the postsynaptic membrane, where they bind to nicotinic receptors and elicit the opening of the receptors’ cation channels. Upon channel opening by ACh, the membrane conductance increases, the membrane depolarizes, and an action potential may be generated indirectly by activation of voltage-gated Na^+ and K^+ channels. In muscle, this action potential is conducted to the transverse tubule system where release of Ca^{2+} into the sarcoplasm leads to muscle contraction. As in muscle, stimulation of nicotinic receptors in neuronal tissue may result indirectly in the generation of action potentials, which can be transmitted to distant parts of the neuron. In addition, certain neuronal nicotinic receptor-ion channels are highly permeable to Ca^{2+} , and stimulation of such receptors located on tiny neuronal structures, including dendritic spines and axon terminals, may change extracellular and/or intracellular Ca^{2+} concentrations sufficiently to modulate other Ca^{2+} -dependent mechanisms. Thus, the important role of the neuronal nicotinic receptors in plasticity and cognition may lie partly in their ability

to modulate Ca^{2+} -triggered and second-messenger mediated intracellular processes such as transmitter release, long-term potentiation, and gene expression, as well as to regulate the function of nearby ligand-gated receptors. The homology among the subunits of muscle and neuronal types of nicotinic receptors demonstrates a long evolutionary heritage that has preserved the sites for ACh and, in particular, the putative transmitter. Furthermore, nicotinic receptors are part of a larger superfamily of less closely related, transmitter-gated ion channels, including glycine, γ -amino-butyric acid (GABA_A), and serotonin (5-HT_3) receptors. The evolutionary conservation of the structure of these receptors suggests that the basic mechanism by which these receptors accomplish signal transduction may be shared.

2. Structure

The abundance of nicotinic receptors in the electric organs of certain fishes, e.g. *Torpedo californica* and *Torpedo marmorata*, combined with the discovery of α -bungarotoxin (α BGT), a polypeptide from the venom of the snake *Bungarus multicinctus* that is a virtually irreversible ligand and a specific antagonist of ACh at the muscle-type of nicotinic receptor, made possible the biochemical extraction and characterization of the nicotinic receptor and the identification of the ACh-binding site. The receptor was characterized as a heterooligomeric complex of four distinct protein subunits, which are named with Greek letters in order of their molecular size (α , 40 kDa; β , 50 kDa; γ , 60 kDa; and δ , 65 kDa). During natural expression, these subunits are combined intracellularly in α - γ and α - δ dimers, then an α - δ - β trimer is formed, and finally the pentameric receptor is inserted into the membrane with the stoichiometry $\alpha_2\beta\gamma\delta$ (Figure 1). The quaternary molecular structure of the muscle-type receptor has been shown by X-ray crystallographic

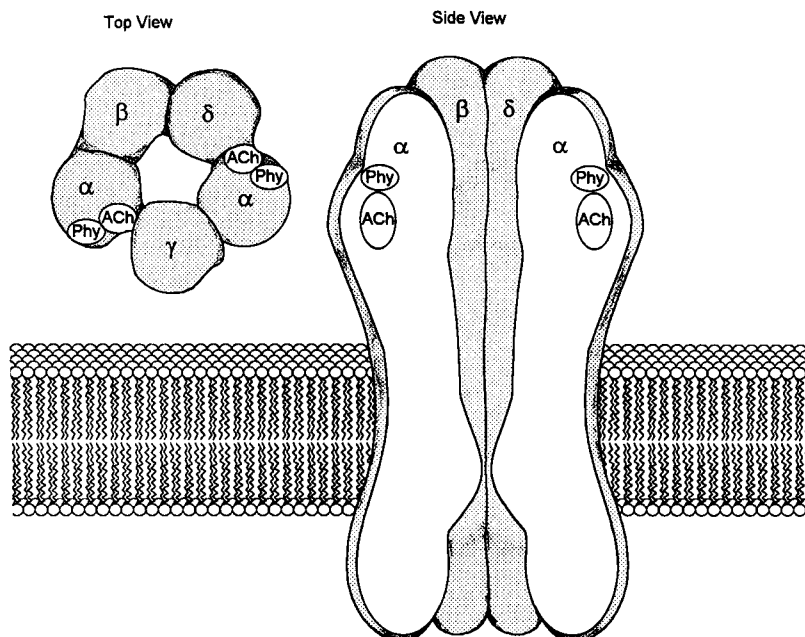


Figure 1. Pentameric structure of the muscle-type nicotinic acetylcholine receptor-ion channel. Each α subunit bears recognition sites for acetylcholine (ACh) and physostigmine (Phy)-like agonists.

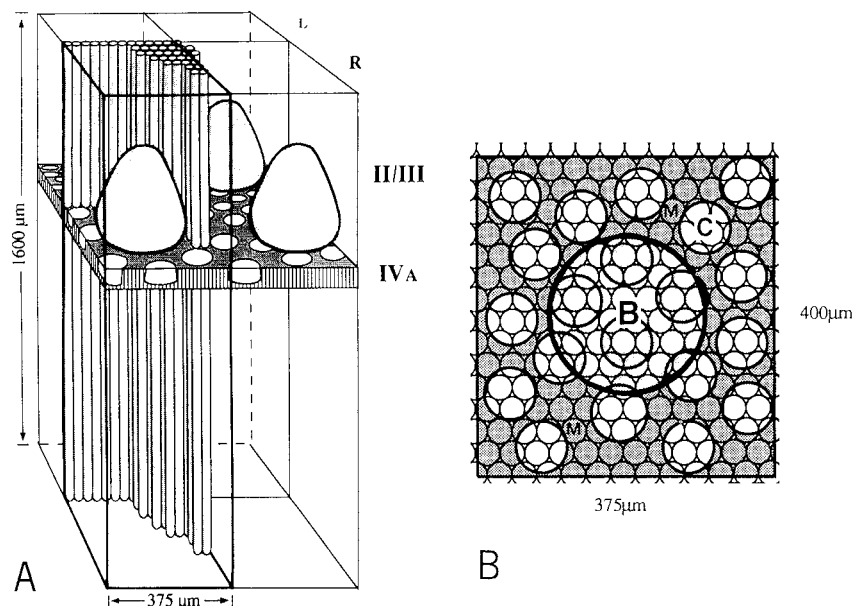


Figure 2. Diagrammatic representation of the relationships between CO “blobs”, layer IV cones, and pyramidal cell modules. “A”, Three-dimensional representation. The “blobs” in layer II/III are aligned in single rows along the 400 μm -wide ocular dominance columns (R and L), and they have a center-to-center spacing of 375 μm . Each blob, which is the focus of a blob-centered module, lies above the cones of neurons in layer IVA, and throughout the entire cortex is a matrix of long, thin pyramidal cell modules. B, a diagram of the contents of a blob-centered module as though looking down from the pial surface. The blobs (B) are about 200 μm wide. An average of 20 layer IVA cones (C) would occupy such an area, which would also contain some 180 pyramidal cells modules (M).

the IVA layer cones and the laminae II/III noncellularly localized cytochrome oxidase (CO) *blobs* are shown in diagram A stereodiagrammatically and in B as if viewed vertically through the pial surface. The whole tissue ensemble is, indeed, a *quasi crystalline structure*.

Wherever researchers have looked for structure and connectivity of neurons in any part of the neocortex and even more so in more archaic cortical parts, they found a hitherto unexpected precision and sophistication of structure and architecture. The expectation that the same types of architectonic would be found – beyond some basic principles, determined by the finite number of cell and dendritic as well as axonal arborization types – across various cortical regions and various species would be absurd, indeed.

References

Purves D, Riddle DR, La Mantia AS (1992): *Trends Neurosci* 15:362–368

Swindale NV (1990): Is the cerebral cortex modular? *Trends Neurosci* 13:487–492

Further reading

- Goldman-Rakic PS, Rakic P, eds. (1991–1994) *J Cereb Cortex* vols. 1–4
 Palay SL, Chan-Palay V, eds. (1982): The cerebellum: New vistas. *Experimental Brain Research, Suppl.* 6. Berlin: Springer-Verlag
 Székely Gy (1979): Does neuronal morphology carry information for the establishment of interneuronal connections? In: *Neural Growth and Differentiation*, Meisami E, Brazier MAB, eds. New York: Raven Press
 Szentágothai J (1978): The neuron network of the cerebral cortex: A functional interpretation. The Ferrier Lecture 1977. *Proc R Soc Lond*
 Szentágothai J (1983): The modular architectonics principle of neural centers. *Rev Physiol Biochem Pharmacol* 98:11–61

See also Brain, hierarchical organization; Brains, structural symmetries of; Cortical motor columns

Artificial intelligence

Daniel Crevier

Artificial intelligence (AI), like the neurosciences, aims at explaining how mind emerges out of matter. Contrary to neurosciences it tries to achieve this goal by building intelligent systems out of computer hardware and software. Will AI just tell us something about computers, or can one expect any cross-fertilization between it and the neurosciences? This survey provides clues on these issues by discussing some of the

potential architectures for intelligent systems under study by the AI community.

1. Goals and schools of AI

The two main goals of AI can be broadly defined as making machines more intelligent and understanding the basic nature

many years after reaching the perikaryon, until replication is reactivated by physiological stress. With herpes, new virions are delivered to terminals by anterograde transport and released, where they cause the characteristic, highly localized skin lesions of shingles or fever blisters that follow the boundaries of dermatomes for infected neurons.

Not all viruses enter the nervous system by retrograde axonal transport. For example, systemic infections can invade if the blood brain barrier becomes leaky. However, when an appropriate binding site is accessible on one or more classes of neuron, retrograde transport provides an efficient and selective pathway for entry into the nervous system.

Acknowledgements The authors would like to thank Dr. Ann Sperry for critical comments on the manuscript. Preparation of this chapter was supported in part by grants from the National Institute of Neurological Disease and Stroke NINDS (NS23868 and NS23320), a joint grant from NASA and the National Institute of Aging (NAG2-962/AG12646), from the Welch Foundation (#1237), and from the Muscular Dystrophy Association.

Further reading

- Brady S (1985): Axonal transport methods and applications. In: *Neuromethods, General Neurochemical Techniques*, Boulton A, Baker G, eds. Clifton, NJ: Humana Press, pp. 419–476
- Heumann R, Korschning S, Bandtlow C, Thoenen H (1987): Changes in nerve growth factor synthesis in nonneuronal cells in response to sciatic nerve transection. *J Cell Biol* 104:1623–1631

- Kristensson K (1970): Transport of fluorescent protein tracer in peripheral nerves. *Acta Neuropathol* 16:293–300
- Kristensson K (1992): Potential role of viruses in neurodegeneraftion. *Mol Chem Neuropathol* 16:45–58
- LaVail JH, LaVail MM (1974): The retrograde intraxonal transport of horseradish peroxidase in the chick visual system: A light and electron microscopic study. *J Comp Neurol* 157:303–358
- LaVail JH, Meade LB, Dawson CR (1991): Ultrastructural immunocytochemical localization of herpes simplex virus (type 1) in trigeminal ganglion neurons. *Curr Eye Res* 10(Suppl):23–29
- Mesulam M (1982): *Tracing Neuronal Connections with Horseradish Peroxidase*. New York: Wiley
- Schmied R, Huang, C-C, Zhang X-P, Ambron DA, Ambron RT (1993): Endogenous axoplasmic proteins and proteins containing nuclear localization sequences use the retrograde axonal transport/nuclear import pathway. *J Neurosci* 13:4064–4071
- Simpson LL (1992): Neurotoxins. In: *Methods in Neuroscience*, Conn MP, ed. New York: Academic Press, pp. 55
- Steward O (1981): Horseradish peroxidase and fluorescent substrates and their combination with other techniques. In: *Neuroanatomical Tract-Tracing Methods*, Heimer L, Robards M, eds. New York: Plenum Press, pp. 279–310
- Stoeckel K, Schwab M, Thoenen H (1975): Comparison between the retrograde axonal transport of nerve growth factor and tetanus toxin in motor, sensory and adrenergic neurons. *Brain Res* 99:1–16
- Stoeckel K, Thoenen H (1975): Retrograde axonal transport of nerve growth factor: Specificity and biological importance. *Brain Res* 85:337–341

See also Axon; Axonal transport; Neurotoxins, neurotoxicology; Neurovirology